DOI: 10.1002/chem.201301124

Catalyst Activity and Selectivity in the Isomerising Alkoxycarbonylation of Methyl Oleate

Josefine T. Christl, Philipp Roesle, Florian Stempfle, Philipp Wucher, Inigo Göttker-Schnetmann, Gerhard Müller,* and Stefan Mecking*[a]

Abstract: The synthesis of unsymmetrical diphosphine ligands (**3a**–**g**) with an *o*-tolyl backbone and *tert*-butyl, adamantyl, cyclohexyl and isopropyl substituents on the phosphorus moiety is described (1,2-$(CH_2PR_2)(PR'_2)C_6H_4$; **3a**: R = *t*Bu, R′ = *t*Bu, **3b**: R = *t*Bu, R′ = Cy, **3c**: R = *t*Bu, R′ = *i*Pr, **3d**: R = Ad, R′ = *t*Bu, **3e**: R = Ad, R′ = Cy, **3f**: R = Cy, R′ = Cy, **3g**: R = Ad, R′ = Ad). The corresponding diphosphine–Pd^{II} ditriflate complexes [(P^P)Pd$(OTf)_2$] (**5a**–**g**) were prepared and structurally characterised by X-ray crystallography. These new complexes were studied as catalyst precursors in the isomerising methoxycarbonylation of methyl oleate, and were found to convert methyl oleate into the corresponding linear α,ω-diester (**L**) with 70–80% selectivity. The products of this catalytic reaction with the known [{1,2-$(tBu_2PCH_2)_2C_6H_4$}Pd$(OTf)_2$] complex (**5h**) were fully analysed, and revealed the formation of the linear α,ω-diester (**L**, 89.0%), the methyl-branched diester **B1** (4.3%), the ethyl-branched diester **B2** (1.0%), the propyl-branched diester **B3** (0.6%) and all diesters from butyl- to hexadecyl-branched diesters **B4**–**B16** (overall 4.8%) at 90 °C and 20 bar CO. The productivity of the catalytic conversion of methyl oleate with complexes **5a**–**g** varied with the steric bulk of the alkyl substituent on the phosphorus. Ligands with more bulky groups, like *tert*-butyl or adamantyl (e.g., **5a**, **5d**, **5g**), were more productive systems. The formation of the catalytically active hydride species $[(P^P)Pd(H)(MeOH)]^+$ (**6-MeOH**) was investigated and observed directly for complexes **5a**–**e** and **5g**, respectively. These hydride species were isolated as the corresponding triphenylphosphine complexes (**6-PPh_3**) and fully characterised, including by X-ray crystallography. The catalytic productivity of **6a-PPh_3** was virtually identical to that of **5a**, thereby confirming the efficient hydride formation of **5a** under catalytic conditions.

Keywords: carbonylation · isomerisation · palladium · phosphines · renewable resources

Introduction

The use of renewable resources as a source of chemicals requires their efficient transformation into useful building blocks. Fatty acids are attractive feedstocks due to their unique, long-chain methylene sequences.[1] Their transformation into linear, α,ω-functionalised compounds is of interest, for example, for the generation of semi-crystalline aliphatic polyesters and hydrophobic polyamides. The terminal functionalisation of fatty acids is a synthetic challenge, however. Biotechnological[2,3] as well as entirely chemical catalytic approaches[1b,4] are studied to this end.

Alkoxycarbonylation of ethylene to methyl propionate has recently been implemented as a part of a new industrial process to methyl methacrylate developed by Lucite International.[5,6] This reaction is catalysed with high rates by palladium(II) complexes of 1,2-$(tBu_2PCH_2)_2C_6H_4$ (dtbpx; "Lucite ligand").[7]

Remarkably, palladium(II) catalysts modified with *meso*/*rac*-1,3-bis(phospha-oxa-adamantyl)propane[8a] or the aforementioned diphosphine dtbpx[8b] (Figure 1) convert the double bond of internal olefins into a terminal ester group. Thus, the double bond deep in the chain of unsaturated fatty acids is carbonylated to a terminal ester group with high selectivity, yielding α,ω-diesters.[9–11] These α,ω-diesters can be converted into α,ω-diols, α,ω-diamines and α,ω-ace-

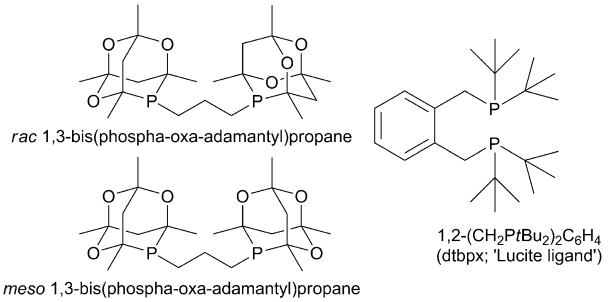

Figure 1. Bulky diphosphine ligands that convert internal octenes into linear esters.

[a] M.Sc. J. T. Christl, M.Sc. P. Roesle, M.Sc. F. Stempfle, Dipl.-Chem. P. Wucher, Dr. I. Göttker-Schnetmann, Prof. Dr. G. Müller, Prof. Dr. S. Mecking
Department of Chemistry, University of Konstanz
78464 Konstanz (Germany)
Fax: (+49) 7531-88-5152
E-mail: gerhard.mueller@uni-konstanz.de
stefan.mecking@uni-konstanz.de

Supporting information for this article is available on the WWW under http://dx.doi.org/10.1002/chem.201301124.

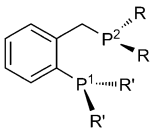

Figure 2. Unsymmetrical diphosphine ligands synthesised in this work. **3a**: R = *t*Bu, R′ = *t*Bu, **3b**: R = *t*Bu, R′ = Cy, **3c**: R = *t*Bu, R′ = *i*Pr, **3d**: R = Ad, R′ = *t*Bu, **3e**: R = Ad, R′ = Cy, **3f**: R = Cy, R′ = Cy, **3g**: R = Ad, R′ = Ad.

tals, all obtained in polycondensation-grade purity (>99%).[12] Beyond these findings, no further insights into the requirement of diphosphine ligands to promote this unusual catalytic isomerising alkoxycarbonylation have been reported. To this end, we chose the *o*-tolyl backbone[13,26] (Figure 2) as this allows for more straightforward and less hazardous preparation of diphosphines in comparison with 1,2-(tBu$_2$PCH$_2$)$_2$C$_6$H$_4$. More importantly, a large range of unsymmetrically substituted, bulky electron-rich diphosphines are also accessible selectively.[13,14] We report herein on the corresponding neutral complexes suitable as single-component catalyst precursors, and their selectivity in isomerising methoxycarbonylation reactions.

Results and Discussion

The isomerising methoxycarbonylation of methyl oleate (MO) or the corresponding triglyceride has been reported to yield dimethyl nonadecane-1,19-dioate (**L**) as the major product, which can be obtained cleanly (see above).[10–12] However, a comprehensive picture of the selectivity and the products formed remains to be established. By crystallisation of the crude reaction mixture from methanol (used as the reaction medium in catalysis), the desired linear product **L** is obtained in >99% purity (Figure 3).[12a,b] As a prerequisite for a correlation of diphosphine ligand structure with selectivity, a detailed analysis of the products of isomerising methoxycarbonylation with [(dtbpx)Pd(OTf)$_2$] (**5h**) was performed.

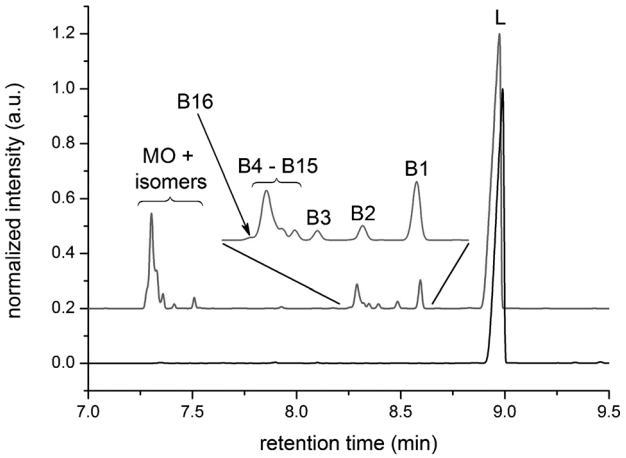

Figure 3. Comparison of the gas chromatograms of the crude reaction mixture (top) and after crystallisation from methanol (bottom) of the products obtained in the isomerising methoxycarbonylation of methyl oleate with [(dtbpx)Pd(OTf)$_2$] (**5h**) (MO/Pd = 500, 120 h, 20 bar CO, 90 °C).

Products of the isomerising methoxycarbonylation of methyl oleate: The product spectrum formed was determined from a reaction in which [(dtbpx)Pd(OTf)$_2$] (**5h**) was used as the defined catalyst precursor[12b] with a ratio of methyl oleate/Pd of 500 and a prolonged reaction time of 120 h at 90 °C at a CO pressure of 20 bar using a mechanically stirred (500 rpm) 200 mL pressure reactor. Pure methyl oleate (99%) was used to exclude impurities from the starting material and facilitate identification of the products. GC analysis revealed a MO conversion of 80.9%. As no saturated monoesters as side-products (methyl stearate) were observed, we concluded that MO is converted exclusively into diesters by reaction of its double bond with CO and MeOH. Besides the desired product (dimethyl nonadecane-1,19-dioate, **L**), formed in a total yield of 71.8%, 16 branched diester (by-)products (**B1**–**B16**) are conceivable with MO as the starting material (Scheme 1). In these byproducts, the newly formed ester function is not at the ω position, but at all positions from ω−1 (**B1**) to the α (**B16**) position. GC analysis (Figure 3) of the crude reaction mixture showed that at least seven branched esters are formed (see the Supporting Information). To identify the byproducts, these were enriched by removing the linear dimethyl nonadecane-1,19-dioate (**L**) from the crude reaction mixture by crystallisation from methanol and column chromatography of the supernatant to remove the starting material (MO; for details, see

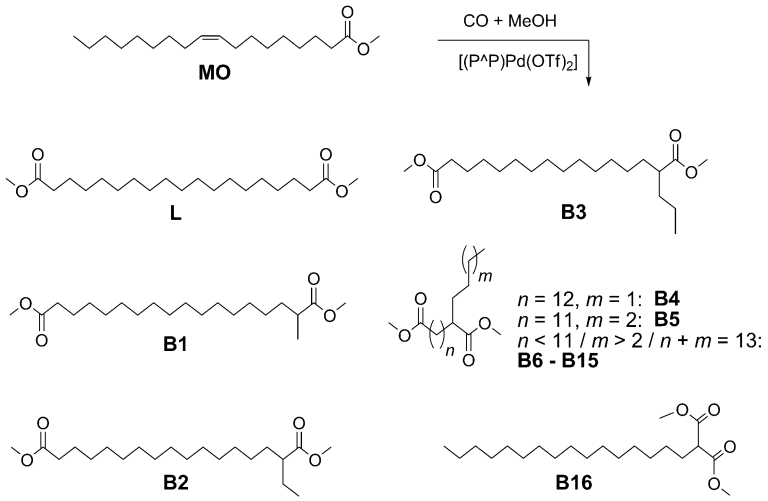

Scheme 1. Possible products formed during the isomerising methoxycarbonylation of methyl oleate.

the Supporting Information). NMR analysis (^{1}H, ^{13}C, ^{1}H,^{1}H COSY, ^{1}H,^{13}C HSQC, ^{1}H,^{13}C HMBC) of this purified reaction mixture revealed the presence of dimethyl 2-methyloctadecane-1,18-dioate (**B1**), dimethyl 2-ethylheptadecane-1,17-dioate (**B2**) and dimethyl 2-propylhexadecane-1,16-dioate (**B3**). Longer-chain branched diesters, dimethyl 2-butylpentadecane-1,15-dioate (**B4**) and dimethyl 2-pentyltetradecane-1,14-dioate (**B5**), were also found. For diesters with even longer branches, **B6**–**B15**, individual compounds could not be assigned unambiguously by NMR spectroscopy.

Formation of the malonic ester MeOOC-CHR-COOMe (R = $C_{16}H_{33}$; **B16**) was evidenced by comparison with the ^{13}C carbonyl NMR shift of a genuine sample of the compound prepared independently, and also by enrichment of the purified reaction mixture with this genuine sample in the GC analysis (see the Supporting Information).

Table 1 gives the product distribution as determined by GC. The selectivity for the formation of the linear diester dimethyl nonadecane-1,19-dioate (**L**) was found to be 89.0%. Amongst the branched products, dimethyl 2-methyloctadecane-1,18-dioate (**B1**) predominates with 4.3% content. The portion of the respective branched products decreases with increasing length of the branch. The malonic diester (**B16**) is also formed, but to a very small extent only. This is in accordance with our recent mechanistic studies[9] by low-temperature NMR spectroscopy and DFT methods in which a preference for linear insertion products along with a roughly similar amount of the branched acyl [(P^P)PdC(=O)CHRCOOMe]$^+$ was observed. The formation of the latter is promoted by the stabilisation incurred by chelation of the ester group of the MO substrate. However, this branched acyl is subject to a relatively slow methanolysis, and thus only a very small amount of **B16** was formed.

Table 1. Product distribution observed in the isomerising methoxycarbonylation of methyl oleate with [(dtbpx)Pd(OTf)$_2$].[a]

Product	L	B1	B2	B3	B4–B15	B16
Fraction [%]	89.0	4.3	1.0	0.6	4.8	0.3

[a] Reaction conditions: 96 mmol (28.5 g) MO (99%), 0.19 mmol (153 mg) [(dtbpx)Pd(OTf)$_2$], 130 mL MeOH, 20 bar CO, 90°C, 120 h. Total conversion of MO was 80.9%. Product distribution calculated from GC data.

Synthesis of the diphosphine ligands: Pd^{II} complexes bearing the sterically demanding 1,2-(tBu$_2$PCH$_2$)$_2$C$_6$H$_4$ ligand are known to be very productive in the isomerising alkoxycarbonylation of plant oils[10,11,12a,b] but the diphosphine is somewhat hazardous to synthesise, especially when sodium alkyl intermediates are involved.[15] Following the rationale of using bulky substituents on phosphorus and a relatively rigid backbone, we chose the *o*-tolyl backbone to vary the substituents at both phosphorus atoms independently in nonsymmetric diphosphines. At the same time, the target ligands are conveniently accessible in three steps from commercially available *o*-bromobenzyl bromide (**1**) as the starting material (Scheme 2). Compound **1** was treated with secondary bulky phosphines such as HP(tBu)$_2$, HP(Ad)$_2$ or HP(Cy)$_2$, leading to the corresponding monosubstituted intermediate derivatives as hydrobromic acid salts, which precipitate as white solids. The best yields were obtained with acetonitrile as a solvent. After the subsequent release of hydrobromide, the resulting neutral monophosphines **2a**, **2d** and **2f** could be used directly in the next step without further purification (purity by ^{1}H NMR, >98%).

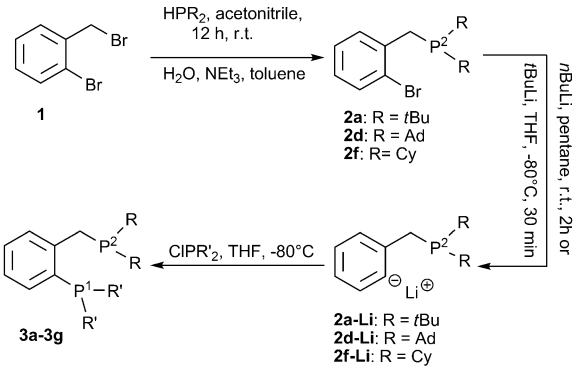

Scheme 2. Synthetic route to the unsymmetrical diphosphines. **3a**: R = tBu, R′ = tBu; **3b**: R = tBu, R′ = Cy, **3c**: R = tBu, R′ = iPr, **3d**: R = Ad, R′ = tBu, **3e**: R = Ad, R′ = Cy, **3f**: R = Cy, R′ = Cy, **3g**: R = Ad, R′ = Ad.

Compound **2a** was lithiated in pentane by the addition of nBuLi at room temperature over 2 h. The corresponding isolated lithium aryl **2a-Li** was treated with chlorophosphines in THF at −80°C to afford the desired unsymmetrical diphosphines **3a** and **3b**, which were recrystallised from ethanol.

Alternatively, the monophosphines **2a**, **2d** and **2f** were lithiated in THF solution with tBuLi at −80°C. The in situ generation of the lithium aryls of the monophosphines turned out to be advantageous due to the limited stability of the isolated lithium aryls. By using tBuLi as the lithiation agent rather than nBuLi, the in situ formation of the lithium aryl occurred more rapidly. The target compounds **3c**–**f** were obtained in moderate-to-high yields (34–87%) by quenching the in situ generated lithium aryls with chlorophosphines followed by recrystallisation from ethanol, leading to suitable crystals of diphosphines **3a**, **3d** and **3f** for X-ray diffraction (see the Supporting Information). To further explore the potential of bulky alkyl substituents, another chelating ligand with two adamantyl groups on both phosphorus atoms was synthesised. The general synthetic route led to diphosphine **3g** but by using the corresponding bromophosphine BrPAd$_2$[23] instead of the chlorophosphine. BrPAd$_2$ was prepared by the reaction of HPAd$_2$ with CBr$_4$ in CH$_2$Cl$_2$. The reaction took place within several minutes at room temperature. The desired bromo compound was isolated in 95% yield by removing the solvent in vacuum. In situ lithiation of **2d** and addition of BrPAd$_2$ led to the formation of **3g**, which was isolated after several crystallisation steps from MeOH and pentane.

Table 2. $^{31}P\{^1H\}$ NMR chemical shifts of the diphosphine ligands **3a–f**.[a]

Ligand	**3a** *t*Bu/*t*Bu	**3b** *t*Bu/Cy	**3c** *t*Bu/*i*Pr	**3d** Ad/*t*Bu	**3e**[b] Ad/Cy	**3f** Cy/Cy	**3g**[b] Ad/Ad
$\delta(P^2)$ [ppm]	35.0	36.4	36.4	33.8	38.1	7.9	35.9
$\delta(P^1)$ [ppm]	15.0	−17.6	−8.7	13.6	−17.7	−16.1	16.1

[a] In C_6D_6 at 25 °C, unless noted otherwise. [b] In $CDCl_3$.

The ^{31}P NMR shifts of the diphosphine ligands (Table 2) show good correlation with the nature of the substituents R and R′, with δ decreasing in the order $t\text{Bu} \approx \text{Ad} > i\text{Pr} > \text{Cy}$.

Synthesis and molecular structures of the diphosphine–Pd^{II} complexes: The desired Pd^{II} complexes were obtained by a two-step protocol starting from the diphosphine ligands and [Pd(dba)$_2$] (Scheme 3).[9,27] The diphosphine (**3a–g**) and [Pd(dba)$_2$] were mixed in THF and stirred at room temperature for 12 h. After filtration of small amounts of palladium

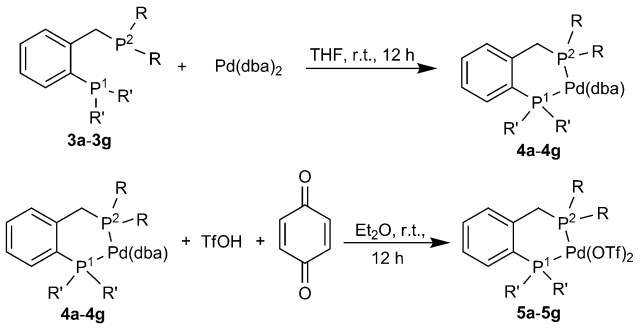

Scheme 3. Synthesis of diphosphine–Pd^{II} complexes **5a–g**.

black and removal of the solvent, the reddish residue obtained was washed with pentane to remove residual diphosphine. The obtained diphosphine–Pd^0 complexes were used in the next step without characterisation. Crystals of **4d** suitable for X-ray crystallography were obtained by the addition of pentane to a solution of **4d** in CH_2Cl_2 (see the Supporting Information).

Dissolution of the [(P^P)Pd^0(dba)] complexes in diethyl ether and addition of trifluoromethanesulfonic acid in the presence of benzoquinone as oxidising agent afforded the desired diphosphine–Pd^{II} ditriflate complexes (**5a–g**) as off-white to yellow solids within 12 h. The complexes were analysed by NMR spectroscopy, X-ray crystallography (Figure 4),[29] mass spectrometry and elemental analysis. Single crystals suitable for X-ray diffraction were obtained by slow diffusion of pentane into methylene chloride solutions of the complexes. Complexes **5a** and **5f** crystallised with 1 equivalent of CH_2Cl_2, and complex **5e** includes half an equivalent of pentane per formula unit in the crystal. All the complexes **5a–f** have four-coordinate Pd^{II} centres that are essentially square planar with tetrahedral distortion in some cases (deviations from the least-root mean-square planes defined by the central metal atom and the four coordinating atoms are given in the Supporting Information). The coordination geometries contain the two phosphorus atoms of the chelating phosphines with the other two coordination sites occupied by triflate oxygen atoms in **5a–c** and **5e**,**f**. In complexes **5b**, **5c**, **5e** and **5f**, both triflate counter anions are coordinated to Pd^{II} in a monodentate fashion, whereas in **5a** (with the $t\text{Bu}_2/t\text{Bu}_2$-substituted diphosphine) only one triflate anion coordinates to palladium as a bidentate chelating ligand. In **5d** ($\text{Ad}_2/t\text{Bu}_2$-substituted diphosphine), only one triflate anion is coordinated as a monodentate ligand, with the fourth coordination site occupied by a water molecule, probably originating from traces of water in the solvent or the trifluoromethanesulfonic acid reagent. Complexes **5d** and **5e** show the most severe deviation from the square-planar geometry (see the Supporting Information). Although the water oxygen atom in **5d** is roughly coplanar with the phosphorus and palladium atoms, the triflate oxygen is situated markedly above this plane. Note that the water oxygen is located *cis* to the -$CH_2P^2Ad_2$ phosphorus atom, whereas the triflate ligand is *cis* to the ArP^1tBu_2 phosphorus atom. This geometrical arrangement seems to be dictated by steric pressure although an intramolecular hydrogen bond between one water hydrogen and a triflate oxygen atom may also play a role (d(O···O) = 2.7(2) Å, ∢ O-H-O 157.1(3)°). Bond lengths and angles (see the Supporting Information) are in the typical range for this type of complex. Interestingly, no clear-cut correlation between steric bulk of the phosphine ligands and the Pd–P bond lengths is evident. In some cases significant differences in aryl/alkyl substituents can be found but no general trend can be easily ascertained. The steric bulk seems to be relieved by a tilt of the P_2Pd and O_2Pd molecular planes with respect to each other (**5a** ($t\text{Bu}_2/t\text{Bu}_2$ substitution at P): ca. 8.4°, **5b** ($t\text{Bu}_2/\text{Cy}_2$): ca. 21.0°, **5c** ($t\text{Bu}_2/i\text{Pr}_2$): ca. 25.5°, **5d** ($\text{Ad}_2/t\text{Bu}_2$): ca. 31.6°, **5e** ($\text{Ad}_2/\text{Cy}_2$): ca. 30.9°, **5f** ($\text{Cy}_2/\text{Cy}_2$): ca. 9.9°). The bite angles[24] of the diphosphine ligands at Pd^{II} range between 89.35(2) and 94.65(5)° (see the Supporting Information).[16] These values are similar to those of dppp and dppf Pd^{II} complexes (91 and 96°, respectively).[28] The complex with the "Lucite ligand" with its more flexible xylyl-type backbone (seven-membered chelate ring) has a slightly higher bite angle of 99.3°.[12b]

Methoxycarbonylation of methyl oleate (MO): The catalytic properties of the new complexes **5a–g** in the isomerising methoxycarbonylation of methyl oleate were then studied (Scheme 4). A constant pressure of CO (20 bar), n(Pd) = 0.048 mmol, n(MO) = 6 mmol, 10 mL methanol, 90 °C and a reaction time of 120 h were chosen as the experimental parameters to evaluate the catalytic performance of com-

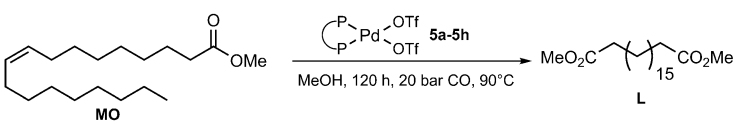

Scheme 4. Methoxycarbonylation of methyl oleate (MO).

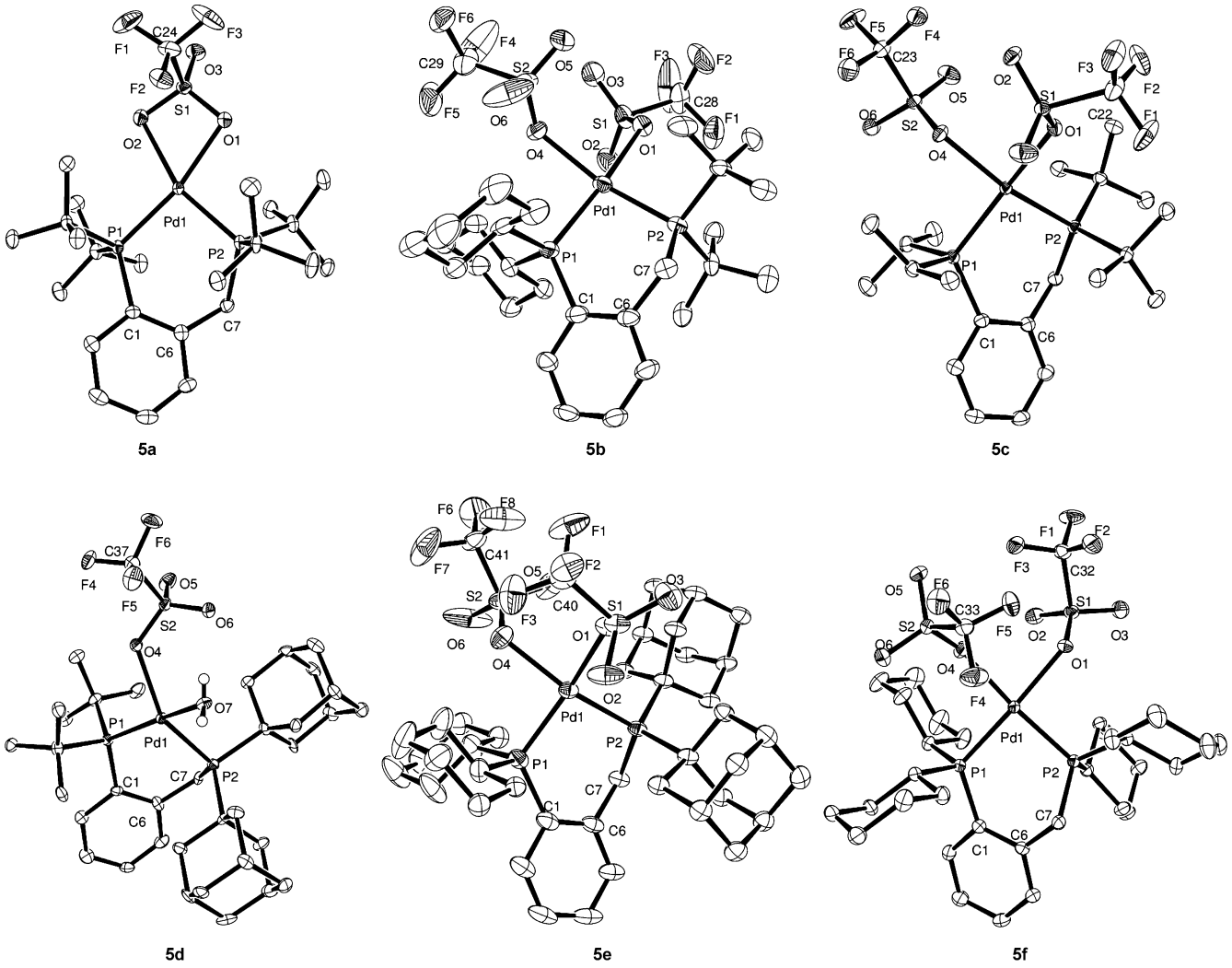

Figure 4. X-ray crystal structures of complexes **5a–f**. Hydrogen atoms except for coordinated H_2O, non-coordinating triflate counter ions, and interstitial solvent molecules have been omitted for clarity. Displacement ellipsoids are shown at the 50% probability level.[29]

plexes **5a–g**. To study the "real-life" catalytic performance, technical-grade Dakolub MB 9001 high oleic sunflower oil methyl ester with a methyl oleate content of 92.5% was used[21] rather than highly pure methyl oleate (Table 3).

Catalysts **5a–g** converted methyl oleate into diesters in yields of 18–98%. Surprisingly, the selectivity towards the desired 1,19-diester was similar (70–80%) for all catalysts studied, however, the conversion varied strongly. Complex **5f** showed a very low conversion (1.3%) of methyl oleate, which is in line with the observation that no hydride formation occurred upon addition of methanol to this complex (see below). The differences in the conversions of **5a–g** can be related to the steric demand of the substituents on the phosphorus moieties of the ligands. To this end, we quantified the available space around the metal centre from the available X-ray crystal structure data (see above). For this purpose we determined the angles between the vector ***V*** defined by the

Table 3. Results of the isomerising methoxycarbonylation of methyl oleate using Pd^{II} complexes **5a–g** and the reference complex **5h**.[a]

Pd^{II} complex	Conversion of MO [%]	Relative distribution [%] 1,19-diester	branched products	Selectivity for linear 1,19-diester [%]
5a (*t*Bu/*t*Bu)	94.2	64.0	30.1	68.0
5b (*t*Bu/Cy)	17.8	13.5	4.3	76.0
5c (*t*Bu/*i*Pr)	18.7	14.0	4.7	75.0
5d (Ad/*t*Bu)	77.4	61.0	16.3	79.0
5e (Ad/Cy)	22.2	17.7	4.5	80.0
5f (Cy/Cy)	1.3	–	–	–
5g (Ad/Ad)	97.1	76.0	20.8	79.0
5h (dtbpx)	95.8	86.8	9.0	90.6

[a] Reaction conditions: n(Pd) = 0.048 mmol, 2 mL Dakolub MB 9001 (92.5% MO), 10 mL MeOH, 20 bar CO, 90 °C, 120 h.

centre between the two phosphorus atoms and the Pd^{II} centre, and four vectors $\boldsymbol{R}_1$, $\boldsymbol{R}_2$, $\boldsymbol{R}_3$ and $\boldsymbol{R}_4$ defined by the Pd^{II} centre and the substituents on the phosphorus moiety (cf. Figure 5). The arithmetic average of these angles is the

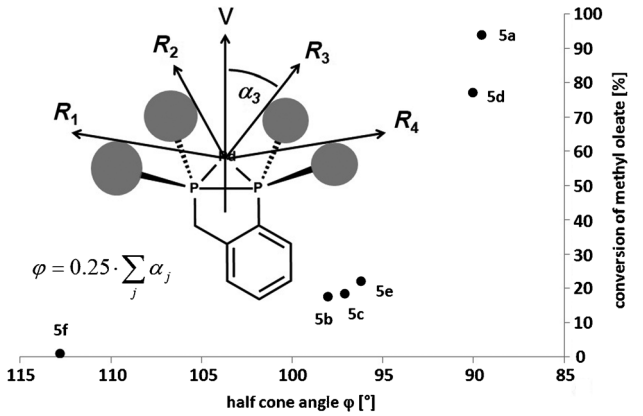

Figure 5. Plot of the conversion of methyl oleate versus the calculated half-cone angle.

"half-cone angle" (for details see the Supporting Information). Note that the angles were calculated from the corresponding X-ray structures without considering the rotation of alkyl substituents around the P–C bond in solution. Larger values indicate increasing available space around the metal centre and thus a smaller steric constraint imposed by the diphosphine ligand. Figure 5 shows the conversion of methyl oleate versus the increasing steric constraint imposed by the diphosphine ligand: increasing conversion accompanies increasing steric demand (**5f**<**5b**<**5c**<**5e**<**5d**<**5a**). The most active unsymmetrical catalysts (**5a** and **5d**, 89 and 90°, respectively) have similar half-cone angles to **5h** (86°).

A more detailed analysis of the relative distribution of the branched ester byproducts (Table 4) shows that catalysts with similar productivity (**5a**, **5d**, **5g** and **5h** versus **5b**, **5c** and **5e**) also show similar distribution of branched products. The less active catalysts have a stronger preference for the methyl-branched product (**B1**), which is the predominant branched ester in all cases, whereas the more bulky substituted and more active catalysts (**5a**, **5d**, **5g** and **5h**) have a lower preference for this methyl-branched product compared with the other branched byproducts.

Table 4. Relative distribution of branched ester byproducts with different catalysts.

Pd^{II} complex	B1	B2	B3	B4–B16
5a (*t*Bu/*t*Bu)	21	3	3	63
5b (*t*Bu/Cy)	49	5	5	41
5c (*t*Bu/*i*Pr)	49	4	4	43
5d (Ad/*t*Bu)	28	3	3	66
5e (Ad/Cy)	51	4	4	41
5g (Ad/Ad)	24	3	3	70
5h (dtbpx)	34	9	6	51

Time dependency of the methyl oleate conversion: Complexes **5a**, **5g** and the reference complex **5h** afforded nearly complete conversion under the studied reaction conditions (120 h). To further evaluate the productivity of these complexes, the conversion with complexes **5a** and **5h** as catalyst precursors was monitored over time. Reactions were carried out in a 200 mL pressure reactor equipped with a sampling valve at the bottom of the reactor from which samples were taken at regular intervals (for details see the Supporting Information). A constant 20 bar pressure of CO, $n(Pd) = 0.77$ mmol, $n(MO) = 96$ mmol, 110 mL methanol and 90 °C were employed with technical-grade Dakolub MB 9001 used as the MO source. Figure 6 shows the consumption of methyl oleate versus time for both complexes **5a** and **5h**.

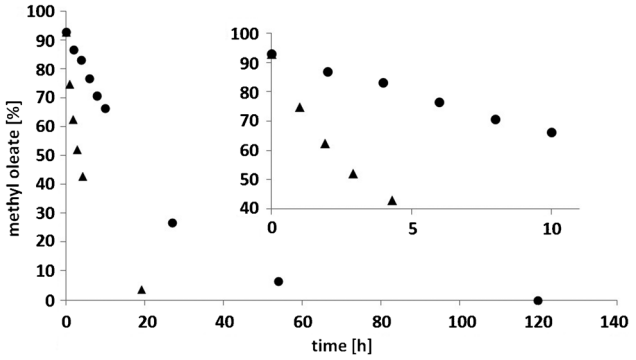

Figure 6. Time dependency of methyl oleate conversion with complexes **5a** (●) and **5h** (▲). Reaction conditions: $n(Pd) = 0.77$ mmol, 32.5 mL Dakolub MB 9001 (92.5% MO), 110 mL MeOH, 20 bar CO, 90 °C.

Although the consumption of methyl oleate with catalyst **5a** is around three times slower than with **5h**, both catalysts eventually completely converted methyl oleate into diesters. The selectivity towards the desired 1,19-diester was 68% for **5a**, and 91% for **5h**, respectively, which agrees with the results of the aforementioned screening of the catalysts under slightly different reaction conditions.

Interestingly, in samples drawn from the reaction with **5h** as a catalyst, considerable amounts of palladium black were observed after a reaction time of 1 h. In contrast, in reactions with **5a**, almost no palladium black was observed. This suggests that catalyst **5a** is more stable towards degradation. Note that the selectivity towards the 1,19-diester is constant over time for both complexes **5a** and **5h**. This implies that any degradation does not impact the nature of the active species.

Formation and isolation of palladium(II) hydride species: The catalytically active species of the methoxycarbonylation reaction is considered to be a Pd^{II} hydride species that is formed within several minutes upon addition of methanol to the [(P^P)Pd(OTf)$_2$] complexes at room temperature.[9,22,27a] To elucidate whether the new Pd^{II} complexes studied here form hydride species upon addition of methanol, complexes

5a–h were dissolved in CD_2Cl_2/MeOH (2:3, v/v) and ^1H and $^{31}P\{^1H\}$ NMR spectra were recorded. Complete conversion of **5a**, **5d**, **5g** and **5h** was revealed by $^{31}P\{^1H\}$ NMR spectroscopy. Evidence for the formation of hydride species arises from the appearance of ^1H resonances at around $\delta = -10$ ppm with typical coupling patterns of diphosphine–Pd^{II} hydride species. Figure 7 exemplarily illustrates the formation of the hydride **6d-MeOH** from **5d** in CD_2Cl_2/MeOH solution. In the ^1H NMR spectrum, a hydride resonance at $\delta =$

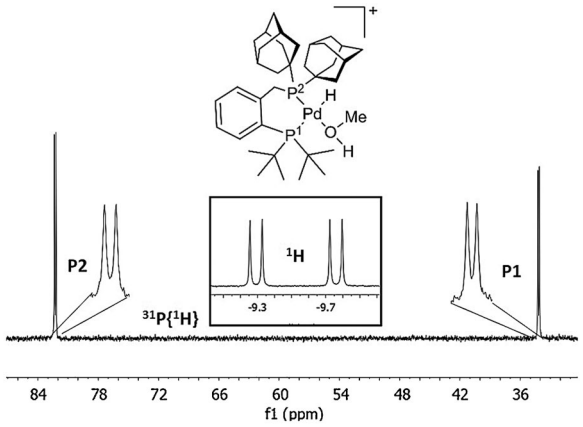

Figure 7. $^{31}P\{^1H\}$ NMR spectrum of the in situ formation of the Pd^{II} hydride species from **5d** in CD_2Cl_2/MeOH (2:3, v/v) at 25 °C. Inset: Pd–H resonances.

−9.53 ppm (doublet of doublets with $^2J_{PHtrans} = 187.6$ Hz and $^2J_{PHcis} = 28.7$ Hz) is observed. The $^{31}P\{^1H\}$ NMR spectrum shows two doublets at 34.2 and 82.3 ppm for the two nonequivalent phosphorus atoms with $^2J_{PPcis} = 24.2$ Hz (Table 5). Notably, only a single isomer of the hydride was observed in MeOH solution. 2D ^1H,^{31}P NMR correlation spectroscopy showed that the signal at $\delta = 34.2$ ppm could be assigned to the aryl phosphorus atom (P^1), whereas the signal at $\delta =$ 82.3 ppm displays $^2J_{PH}$ coupling to the benzyl protons and was therefore identified as the benzyl phosphorus atom (P^2).

With $[D_4]$MeOH as solvent, the respective deuteride complexes were formed (Figure 8). The coupling patterns in the

Table 5. $^{31}P\{^1H\}$ NMR data for Pd^{II} hydride complexes **6-MeOH** in CD_2Cl_2/MeOH at 25 °C.

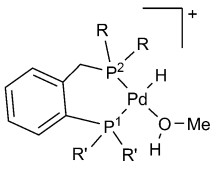

6-MeOH

Pd^{II} hydride	$\delta(P^2)$ [ppm]	$\delta(P^1)$ [ppm]	$^2J(P^2–P^1)$ [Hz]
6a-MeOH (*t*Bu/*t*Bu)	83.8	34.6	24.5
6d-MeOH (Ad/*t*Bu)	82.3	34.2	24.2
6g-MeOH (Ad/Ad)	82.1	33.0	24.3

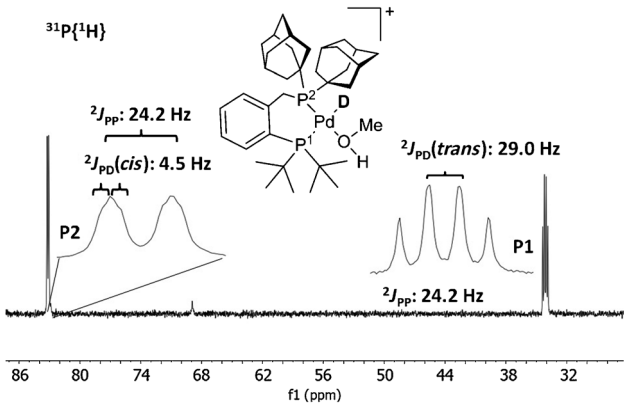

Figure 8. $^{31}P\{^1H\}$ NMR spectrum of the in situ formation of the Pd^{II} hydride species from **5d** in $[D_4]$MeOH at 25 °C.

^{31}P NMR spectrum showed P^2 to be *cis* (doublet of triplet with $^2J_{PPcis} = 24.2$ Hz and $^2J_{PDcis} = 4.5$ Hz) and P^1 to be *trans* (doublet of triplet with $^2J_{PPcis} = 24.2$ Hz and $^2J_{PDtrans} = 29.0$ Hz) to the deuteride. The corresponding observations were made with complexes **5a** and **5g**. The hydride species formed from **5a**, **5d** and **5g** are remarkably stable representatives of Pd^{II} hydrides with a chelating diphosphine ligand and a weakly coordinated solvent molecule. For example, these hydrides can be stored in MeOH at room temperature for 4 or 5 days before decomposition occurs.

In contrast, the addition of methanol to complexes **5b**, **5c** and **5e** did not result in complete conversion of the triflate complexes into single hydride species. Instead, up to 70% (**5e**) of the unreacted triflate complex was still detected. The observation of several ^1H NMR resonances in the region $\delta = -5$ to -10 ppm with different coupling patterns for all three complexes suggests the formation of different hydride species. For complexes **5b** and **5c**, a quintet is observed amongst others, which could indicate the formation of binuclear hydride species.[9] No hydride species were observed from complex **5f** under these conditions.

To isolate the palladium hydrides, we introduced PPh_3 as a strongly coordinating ligand. Addition of PPh_3 to complexes **5a–g** and **5h** in methanol led to the formation of the corresponding $[(P\hat{}P)Pd^{II}(H)PPh_3]^+$ species (**6-PPh$_3$**). Notably, in contrast to the corresponding solvent-coordinated species **6-MeOH**, a mixture of *cis* and *trans* isomers was observed for all complexes, the ratios varying with time. A typical $^{31}P\{^1H\}$ NMR spectrum is shown in Figure 9; all the signals could be assigned to palladium hydrides. In many cases, the predominant isomer is the species with the hydride located *cis* to P^2.

For complexes **5a**, **5d** and **5h**, virtually full conversion to the PPh_3-coordinated hydrides was observed. Although in the cases of **5b**, **5c**, **5e** and **5g** it was possible to form the corresponding PPh_3 hydrides (in yields of 40–90%), the conversion was not enhanced. Signals in the NMR spectra were assigned to the starting triflate complexes.

The hydrides **6a-PPh$_3$** to **6h-PPh$_3$** were isolated by extraction of the methanol solution with pentane, which resulted

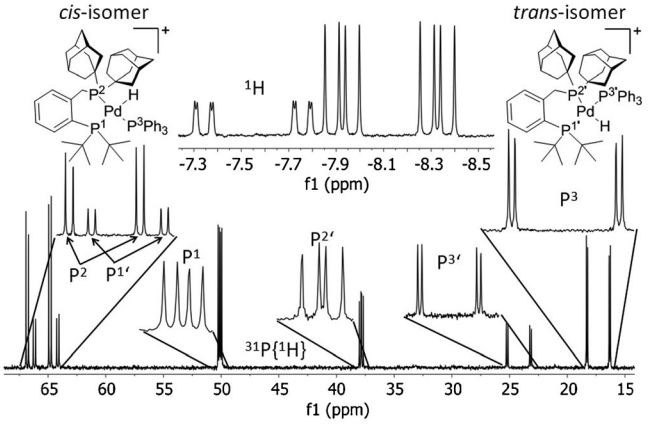

Figure 9. $^{31}P\{^1H\}$ NMR spectrum of **6d-PPh$_3$** formed by dissolution of **5d** and 1 equiv of PPh_3 in CD_2Cl_2/MeOH (2:3, v/v) at 25 °C. Inset: Pd–H resonances.

in precipitation of the desired complexes. Crystals suitable for X-ray diffraction were obtained from **6a-PPh$_3$**, **6e-PPh$_3$**, **6d-PPh$_3$** and **6h-PPh$_3$** by layering a methylene chloride solution of the respective compound with pentane at room temperature (Figure 10). The bond lengths (d(H–Pd) = 1.51(5)–1.54(3) Å) and angles (see the Supporting Information) for **6a-PPh$_3$**, **6e-PPh$_3$** and **6d-PPh$_3$** are in the typical range for this type of complex. In **6a-PPh$_3$** and **6d-PPh$_3$**, the palladium-bound hydrogen is oriented *trans* with respect to P^2, whereas in **6e-PPh$_3$** it is situated *cis*. The different stereochemistry most probably reflects the minimisation of steric hindrance between the PPh_3 ligand and the different steric demands of the R'_2P^1 and $R_2P^2CH_2$ donors. With R = R′ = *t*Bu (**6a-PPh$_3$**) the PPh_3 ligand is oriented *cis* with respect to the more flexible $tBu_2P^2CH_2$ substituent. The same applies to **6d-PPh$_3$** (tBu_2P^1 versus $Ad_2P^2CH_2$), but even a simple inspection of the molecular structure (Figure 10) reveals noticeable distortions arising from the larger steric bulk of the adamantyl substituents. Finally, in **6e-PPh$_3$**, the PPh_3 ligand prefers a *cis* orientation with respect to the (less bulky) Cy_2P^1 group rather than to the $Ad_2P^2CH_2$ moiety, again with severe distortions reflecting the large steric bulk of the groups involved. In **6h-PPh$_3$**, the Pd–H bond length is slightly longer (1.59(2) Å) than in **6a-PPh$_3$**, **6e-PPh$_3$** and **6d-PPh$_3$**.

Upon crystallisation of **6a-PPh$_3$**, which led to the molecular structure shown in Figure 10, crystals of a second species, **7a**, formed. Its structure determination (Figure 10) revealed the formation of a four-membered pallada-phospha-heterocycle formed by C–H activation[25] of the methyl group of a *t*Bu substituent at P^1 by the adjacent palladium centre with the formation of a Pd–C bond (2.120(2) Å) and net expulsion of molecular hydrogen. The preference of a *t*Bu substituent at P^1 for C–H activation over that of a $tBu_2P^2CH_2$ group might again reflect the larger steric rigidity of the R_2P^1 moiety compared with the more flexible $R_2P^2CH_2$ backbone. Probably more important, however, is the *cis* orientation, and thus closer spacial proximity, of the palladium-bound hydrogen atom in **6a** with respect to the activated methyl group of the *t*Bu substituent at P^1 (d(Pd–C15) = 2.120(2) Å). This suggests the direct involvement of the palladium-bound hydrogen atom in the C–H activation process. This formation of a pallada-phospha-heterocycle might also be a part of the deactivation of the catalyst that occurs during the catalytic reaction.

Methoxycarbonylation of methyl oleate with the Pd^{II} hydride species as a catalyst precursor: We conducted methoxycarbonylation experiments of methyl oleate with isolated **6a-PPh$_3$** and **6h-PPh$_3$** as catalyst precursors to probe the possible catalytic productivity of these hydrides. Similar reaction conditions to those used for the methoxycarbonylation reactions with **5a** and **5h** were employed (20 bar CO, ratio (MO/Pd) = 125, 10 mL methanol, 90 °C, 120 h). The catalytic performances of the isolated hydride species are virtually identical to those of the corresponding triflate complexes (Table 6). Although this result may have been anticipated, it is very relevant to confirming the essential issue that hydrides are formed efficiently from the triflate complexes [(P^P)Pd(OTf)$_2$] under catalytic conditions.

Table 6. Comparison of the isomerising methoxycarbonylation of methyl oleate with complexes **5a**, **6a-PPh$_3$**, **5h** and **6h-PPh$_3$**.

Pd^{II} hydride	Conversion of methyl oleate [%]	Relative distribution [%] 1,19-diester	branched products	Selectivity for 1,19-diester [%]
5a (*t*Bu/*t*Bu)[a]	94.2	64.0	30.1	68.0
6a-PPh$_3$[b]	91.0	60.0	30.0	60.0
5h (dtbpx)[a]	95.8	86.8	9.0	90.6
6h-PPh$_3$[b]	97.0	88.6	8.7	91.0

[a] Reaction conditions: n(Pd) = 0.048 mmol, 2 mL Dakolub MB 9001 (92.5 % MO), 10 mL MeOH, 20 bar CO, 90 °C, 120 h. [b] n(Pd) = 0.024 mmol, 1 mL Dakolub MB 9001 (92.5 % MO), 10 mL MeOH, 20 bar CO, 90 °C, 120 h.

Conclusion

Bulky diphosphines **3a–g** with *o*-tolyl backbones have been prepared in moderate-to-good yields. These ligands were transformed into the corresponding diphosphine–Pd^{II} ditriflate complexes **5a–g**. The bite angles of the ligands, as determined by single-crystal X-ray diffraction, are all in the range of 89.35(2)–94.65(5)° for all complexes and similar to the prototypical symmetrical "Lucite ligand" 1,2-(tBu_2PCH_2)$_2C_6H_4$ (99.3°) in **5h**. All the complexes **5a–g** catalysed the isomerising methoxycarbonylation of methyl oleate to yield the linear dimethyl nonadecane-1,19-dioate

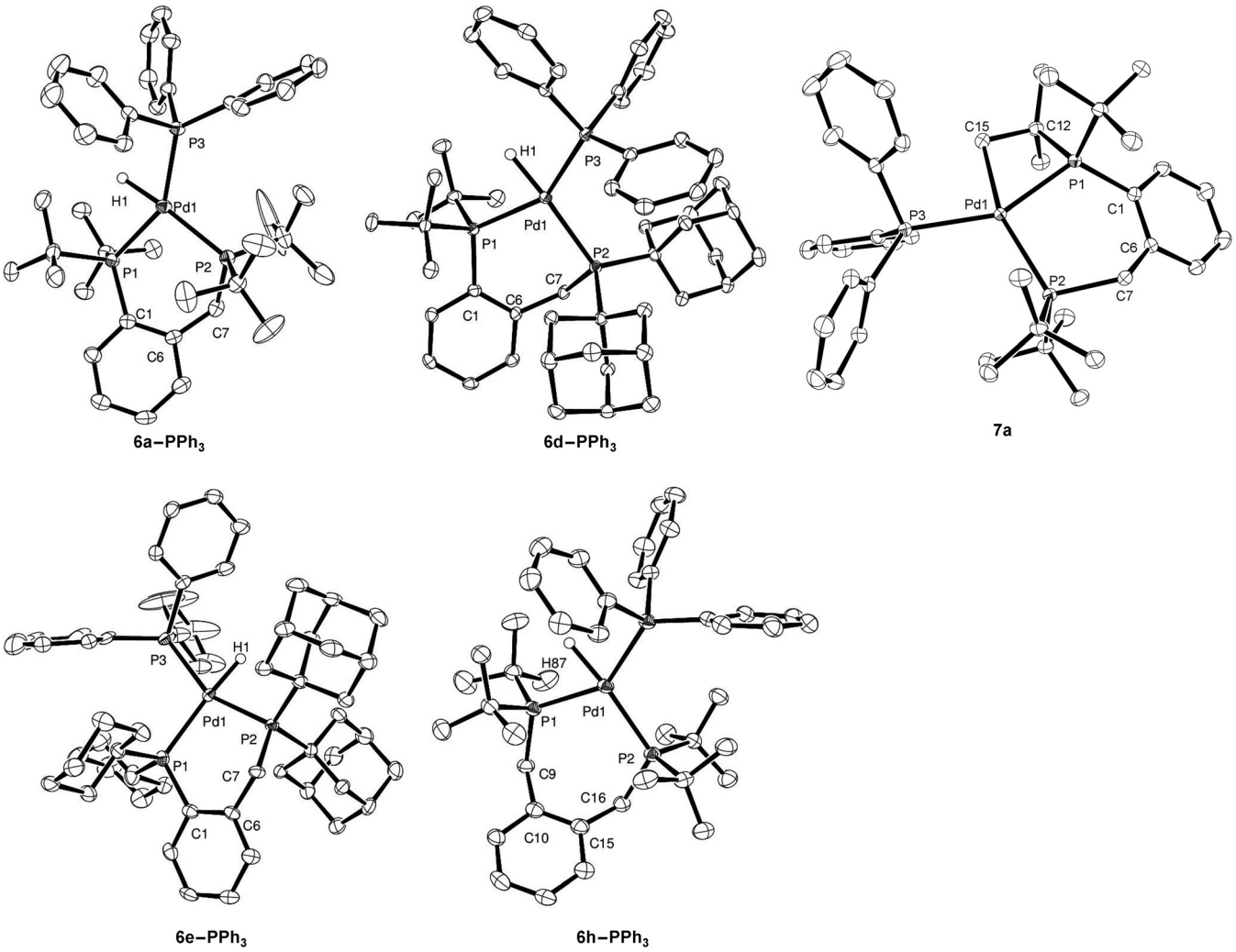

Figure 10. X-ray crystal structures of complexes **6a-PPh$_3$**, **6d-PPh$_3$**, **6e-PPh$_3$**, **6h-PPh$_3$**, and **7a**. Hydrogen atoms (except for Pd–H) and triflate counter ions have been omitted for clarity. Displacement ellipsoids are shown at the 50% probability level.[29]

in moderate-to-good yields. This clearly shows that catalyst **5h** is not unique in transforming the internal double bond deep in the methyl oleate chain into the linear 1,19-diester. A thorough analysis of the products formed revealed that likely all possible branched side-products are formed to a very small extent with the methyl-branched diester predominating significantly compared with the other branched isomers. Remarkably, the selectivity for the linear 1,19-diester over the branched byproducts did not vary strongly for the different diphosphine structures. Also, for less bulky secondary alkyl substituents at the phosphorus, a strong preference for isomerising methoxycarbonylation to the linear product was observed. Structure–productivity relationships were derived from crystallographic and catalytic data. Catalyst productivity clearly increases with steric bulk of the substituents on the phosphorus moiety. Thus, the nature of the bulky substituents at phosphorus appears to influence productivity more distinctly than selectivity. Stoichiometric studies of hydride formation revealed that for the less bulky substituted complexes, formation of the active species is much less efficient than for the *tert*-butyl- and adamantyl-substituted diphosphine. As a guideline for further improving this remarkable and useful reaction, an efficient conversion of a given catalyst precursor into the active species, as well as keeping the latter in the catalytic cycle appear decisive key issues.

Experimental Section

For further details, please see the Supporting Information.

Acknowledgements

Financing by the Stiftung Baden-Württemberg (Programm Umwelttechnologie-forschung, U14) is gratefully acknowledged. P.R. gratefully acknowledges support from the Carl-Zeiss-Foundation through a graduate fellowship. We thank Dako AG for the donation of Dakolub MB 9001. Dr. Etienne Grau is acknowledged for providing complex **6h-PPh$_3$**.

[1] a) U. Biermann, U. Bornscheuer, M. A. R. Meier, J. O. Metzger, H. J. Schäfer, *Angew. Chem.* **2011**, *123*, 3938–3956; *Angew. Chem. Int. Ed.* **2011**, *50*, 3854–3871; b) S. Chikkali, S. Mecking, *Angew. Chem. Int. Ed.* **2012**, *51*, 5802–5808.
[2] a) S. Picataggio, T. Rohrer, K. Deanda, D. Lanning, R. Reynolds, J. Mielenz, L. D. Eirich, *Nat. Biotechnol.* **1992**, *10*, 894–898; b) U. Schörken, P. Kempers, *Eur. J. Lipid Sci. Technol.* **2009**, *111*, 627–645.
[3] W. Lu, J. E. Ness, W. Xie, X. Zhang, J. Minshull, R. A. Gross, *J. Am. Chem. Soc.* **2010**, *132*, 15451–15455.
[4] a) F. Stemple, P. Roesle, S. Mecking, *ACS Symp. Series 1105 Biobased Monomers, Polymers and Materials* (Ed.: R. Gross, P. B. Smith), **2012**, pp. 151–163; b) M. B. Dinger, J. C. Mol, *Adv. Synth. Catal.* **2002**, *344*, 671–677; c) A. Behr, D. Obst, A. Westfechtel, *Eur. J. Lipid Sci. Technol.* **2005**, *107*, 213–219.
[5] a) M. McCoy, J.-F. Tremblay, *Chem. Eng. News* **2009**, *87*, 9; b) B. Harris, *Ingenia* **2010**, *45*, 19–23.
[6] Now: Mitsubishi Rayon; cf. Ref. [5a].
[7] a) W. Clegg, G. R. Eastham, M. R. J. Elsegood, R. P. Tooze, X. L. Wang, K. Whiston, *Chem. Commun.* **1999**, 1877–1878; for a prior report of the coordination chemistry of dtbpx, see: b) N. Carr, B. J. Dunne, A. G. Orpen, J. L. Spencer, *J. Chem. Soc. Chem. Commun.* **1988**, 926–928.
[8] a) R. I. Pugh, E. Drent, P. G. Pringle, *Chem. Commun.* **2001**, 1476–1477; b) C. Jiménez-Rodriguez, D. F. Foster, G. R. Eastham, D. J. Cole-Hamilton, *Chem. Commun.* **2004**, 1720–1721. Also cf; c) V. de La Fuente, M. Waugh, G. R. Eastham, J. A. Iggo, S. Castillón, C. Claver, *Chem. Eur. J.* **2010**, *16*, 6919–6932.
[9] P. Roesle, C. J. Dürr, H. M. Möller, L. Cavallo, L. Caporaso, S. Mecking, *J. Am. Chem. Soc.* **2012**, *134*, 17696–17703.
[10] C. Jiménez-Rodriguez, G. R. Eastham, D. J. Cole-Hamilton, *Inorg. Chem. Commun.* **2005**, *8*, 878–881.
[11] a) G. Walther, J. Deutsch, A. Martin, F. E. Baumann, D. Fridag, R. Franke, A. Köckritz, *ChemSusChem* **2011**, *4*, 1052–1054; b) M. R. L. Furst, R. Le Goff, D. Quinzler, S. Mecking, C. H. Botting, D. J. Cole-Hamilton, *Green Chem.* **2012**, *14*, 472–477.
[12] a) D. Quinzler, S. Mecking, *Angew. Chem.* **2010**, *122*, 4402–4404; *Angew. Chem. Int. Ed.* **2010**, *49*, 4306–4308; b) F. Stempfle, D. Quinzler, I. Heckler, S. Mecking, *Macromolecules* **2011**, *44*, 4159–4166; c) S. Chikkali, F. Stempfle, S. Mecking, *Macromol. Rapid Commun.* **2012**, *33*, 1126–1129; d) F. Stempfle, P. Ortmann, S. Mecking, *Macromol. Rapid Commun.* **2013**, *34*, 47–50.
[13] a) G. R. Eastham, P. I. Richards (Lucite International UK Limited) WO 2009/010782 A1; b) T. Fanjul, G. Eastham, J. Floure, S. J. K. Forrest, M. F. Haddow, A. Hamilton, P. G. Pringle, A. G. Orpen, M. Waugh, *Dalton Trans.* **2013**, *42*, 100–115.
[14] The unsymmetrical diphosphine ligand with four *tert*-butyl substituents (**3a**) has been reported previously, cf. Ref. [13].
[15] A. J. Rucklidge, G. E. Morris, A. M. Z. Slawin, D. J. Cole-Hamilton, *Helv. Chim. Acta* **2006**, *89*, 1783–1800.
[16] They are rather small compared with other diphosphine–Pd^{II} complexes (DPEphos 102.7°, Xantphos 110°) used, for example, in allylic alkylation reactions (see Refs. [17–20]). DPEphos = [oxybis(2,1-phenylene)]bis(diphenylphosphine); Xantphos = 4,5-bis(diphenylphosphino)-9,9-dimethylxanthene.
[17] P. Dierkes, P. W. N. M. van Leeuwen, *Dalton Trans.* **1999**, 1519–1530.
[18] G. P. C. M. Dekker, C. J. Elsevier, K. Vrieze, P. W. N. M. van Leeuwen, *Organometallics* **1992**, *11*, 1598–1603.
[19] J. Ledford, C. S. Schultz, D. P. Gates, P. S. White, J. M. DeSimone, M. Brookhart, *Organometallics* **2001**, *20*, 5266–5276.
[20] P. W. N. M. van Leeuwen, P. C. J. Kamer, J. N. H. Reek, *Pure Appl. Chem.* **1999**, *71*, 1443–14452.
[21] Typical distribution of Dakolub MB 9001: 92.5% methyl oleate, 2.5% methyl linoleate, 2.5% methyl palmitate, 1.5% methyl stearate, 1.0% methyl esters of longer chain ($>C_{18}$) fatty acids.
[22] G. R. Eastham, B. T. Heaton, J. A. Iggo, R. P. Tooze, R. Whyman, S. Zacchini, *Chem. Commun.* **2000**, 609–610.
[23] J. Goerlich, R. Schmutzler, *Phosphorus Sulfur Silicon Relat. Elem.* **1994**, *88*, 241–244.
[24] P. W. N. M. van Leeuwen, *Homogenous catalysis, understanding the art*, Kluwer, **2004**, 125, pp. 16–19.
[25] D. J. Tempel, L. K. Johnson, R. L. Huff, P. S. White, M. Brookhart, *J. Am. Chem. Soc.* **2000**, *122*, 6686–6700.
[26] a) E. Drent, W. W. Jager, R. I. Pugh (Shell Oil Company) US 7265242 B2, **2007**; b) M. Boutain, S. B. Duckett, J. P. Dunne, C. Godard, J. M. Hernández, A. J. Holmes, I. G. Khazal, J. L. Serrano, *Dalton Trans.* **2010**, *39*, 3495–3500; c) A. K. Ghosh, D. R. Nicponski, J. Kass, *Tetrahedron Lett.* **2012**, *53*, 3699–3702; d) M. Davis, F. G. Mann, *J. Chem. Soc.* **1964**, 3786–3790; e) E. Drent, R. Ernst, W. W. Jager, (Shell Internationale Research Maatschappij) WO2004/103948A1.
[27] a) W. Clegg, G. R. Eastham, M. R. J. Elsegood, B. T. Heaton, J. A. Iggo, R. P. Tooze, R. Whyman, S. Zacchini, *Organometallics* **2002**, *21*, 1832–1840; b) J. J. R. Frew, K. Damian, H. Van Rensburg, A. M. Z. Slawin, R. P. Tooze, M. L. Clarke, *Chem. Eur. J.* **2009**, *15*, 10504–10513.
[28] dppp = 1,3-bis(diphenylphosphino)propane; dppf: 1,1′-bis(diphenylphosphino)ferrocene.
[29] CCDC-931019 (**3a**), CCDC-931020 (**3d**), CCDC-931021 (**3f**), CCDC-931022 (**4d**), CCDC-931025 (**5a**), CCDC-931023 (**5b**), CCDC-931024 (**5c**), CCDC-931012 (**5d**), CCDC-931013 (**5e**), CCDC-931014 (**5f**), CCDC-931015 (**6a-PPh$_3$**), CCDC-931016 (**6d-PPh$_3$**), CCDC-931017 (**6e-PPh$_3$**), CCDC-937890 (**6h-PPh$_3$**), CCDC-931018 (**7a**) contain the supplementary crystallographic data for this paper. These data can be obtained free of charge from The Cambridge Crystallographic Data Centre via www.ccdc.cam.ac.uk/data_request/cif. Further details are also given in the Supporting Information.

Received: March 23, 2013
Published online: November 20, 2013

